# A Numerical Study of Forced Convection around a Snow Sleeve in a Cross Flow of Air

C. Zhang, M. Farzaneh and L. Kiss

NSERC / Hydro-Quebec / UQAC Industrial Chair on Atmospheric Icing of Power Network Equipment (CIGELE) and Canada
Research Chair on Engineering of Power Network Atmospheric Icing (INGIVRE)  www.cigele.ca
at Université du Québec à Chicoutimi, QC, Canada

*Abstract —* **Heat transfer from ambient air to snow is a fundamental factor to determine the snow-melting rate and shape-changing of a snow sleeve. This paper presents the result of investigations on the characteristics of forced convection from a snow sleeve in a cross flow of air, especially on the effects due to the roughness of the snow surface and to the non-circular shape of the sleeve.**

**Two-dimensional State Reynolds-Average Navier-Stokes (RANS) simulations are implemented in Fluent to predict the local heat-transfer coefficient distribution along the snow sleeve surface, and subsequently, the overall heat-transfer rate. Firstly, circular and non-circular sleeve shapes were studied. The outer shape of the snow sleeve changes during the melting process due to wind forces, melted water flowing within the snow, etc. A set of ecliptic shapes are investigated and compared with the values from the circular cylinder shape. Secondly, surface roughness on a circular cylinder sleeve was taken into account. A variety of roughness values have been investigated and compared with each other under the same Reynolds number conditions. The computational results show good concordance with the theoretical analyses and experimental data from literature.**

## I. INTRODUCTION

Snow accretion on overhead transmission lines and ground wires can lead to a number of serviceability, safety and mechanical issues. In order to develop methods to prevent snow accretion or shedding from overhead conductors, it is important to estimate the heat transfer and flow characteristics around snow sleeves in relation to various engineering aspects. For example, convective heat transfer plays a significant role in the thermal balance for snow melting and refreezing processes.

The flow around a circular cylinder at high Reynolds number (*Re*) has long been the subject of intense attention from academic and practical points of view. It is concerned with the complicated interaction between the transition and separation of the boundary layer on a rounded surface. A large number of studies have been carried out by numerous investigators, and several empirical correlations have been developed for the heat transfer coefficient.

The local and overall heat transfer coefficient (HTC) can be determined by:

- experiments (e.g. traditional electrical heating method, optical method), or
- numerical calculations (e.g. using finite volume, finite differences or finite element methods)

Giedt (1941) proposed an experimental schema to describe the variation of local HTC along the circumference of a circular cylinder in a cross flow of air[10]. E. Achenbach (1975),

A. Zhukauskas (1985), J. W. Scholten et al (1998) and E. Buyrul (1999) also presented the distribution of local HTC along a circular or elliptical surface by means of well-designed experiments. K. Szczepanik et al. (2004) and Z. Peter (2006) used numerical methods to study the relationship between the local HTC distribution and Reynolds numbers.

A circular cylinder is a most important and typical example. However, a snow sleeve is not a perfect cylinder all the time, so it is necessary to do some specific study on snow sleeves in that respect.

This paper presents the results of a numerical investigation on the effects of special characteristics of a snow sleeve, including surface roughness and non-circular shape, on the local HTC distribution around the sleeve under different wind conditions.

1.Non-circular shape

During the snow melting process the outer shape of the sleeve changes continuously, due to the melted water flow, metamorphism of the ice matrix within the snow, etc.

A set of elliptical cylinders are simulated in a cross flow of air. The numerical results are compared with those for circular cylinder.

2.Roughness

Microreliefs on the snow surface are formed by a process of erosion and snow redeposition by the wind.

Normally, increasing roughness increases the heat transfer rate in the turbulent boundary layer and, in addition, causes the transition from laminar to turbulent layer to occur earlier.

A total of 10 wind scenarios were simulated in Fluent. The wind varies from 1 to 10 m/s, and the Reynolds number from 7400 to 74 000. Three typical scenarios are presented herein.

## II. NUMERICAL METHOD AND MODEL

For numerical solutions of the Reynolds-averaged Navier Stokes equations, a commercial computational fluid dynamic software package, Fluent, was employed. Fluent uses the finite volume method (FVM) to solve sequentially the governing equations. Several turbulence models were used in this study. Among these, the results from the $k\text{-}\omega$ SST model show better agreement compared to experimental data.

The SST $k\text{-}\omega$ turbulence model utilizes a calculation of turbulent viscosity based on the standard $k\text{-}\omega$ model. Thus the closure coefficients and other relations also differ slightly. Nonetheless for the current study, the SST $k\text{-}\omega$ turbulence model is considered the ordinary or unmodified turbulence model.

The flow across the snow sleeve was solved as an incompressible problem with air being the fluid. Pressure discretization was set by using the Standard and others Second Order Upwind. The coupled method was adopted for pressure-velocity coupling.

The two-equation eddy-viscosity turbulence model requires two boundary conditions. The first is satisfied by the turbulence intensity, *I*. To match experimental conditions, the values of *I* at different Reynolds numbers were set as follow:

| Re | I |
|----|---|
| 7407 | 1.6% |
| 29630 | 0.4% |
| 59259 | 3.2% |

The second boundary value can be expressed in various ways such as turbulence scale, dissipation terms, etc. The viscosity ratio was chosen to be $r_\mu = \mu_t/\mu$, and its value was set to 7 according to the Fluent manual instructions.

The snow sleeve was modeled as a circle (ellipse), and a square flow domain was created around the cylinder (Figure 1). The upstream length is 15 times the radius of the cylinder, and the downstream length is 40 times the radius of the cylinder. Only the upper part of the domain was selected in order to save computing resources.
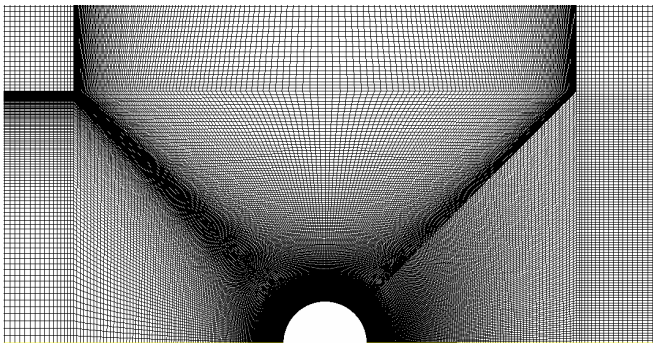


Figure 1. Schema of domain mesh

### III.  FORCED HEAT TRANSFER OF A SMOOTH CIRCULAR CYLINDER

In general, all cases indicate the correct characteristic shape of the local Nusselt number around the circular cylinder. In the subcritical range ($Re<10^5$) a local Nusselt number (*Nu*) maximum is located at or close to the stagnation point. The value of *Nu* then decreases with an increase in θ resulting from the laminar boundary layer development. *Nu* reaches a minimum close to the top of cylinder, at θ≈80°, which is associated with a separation. Moving further into the wake region, *Nu* increases with θ due to the mixing associated with vortex formation.

Figure 2 shows the *Nu* profile from the numerical results for the smooth surface cylinder, i.e. $K_s/d=0$.The horizontal axis is the circumferential angle, in degrees, where 0 degree is the leading edge or front stagnation point of the cylinder, and 180 degrees is its trailing edge or rear. It is assumed that the diameter of the circular cylinder is 0.1m.
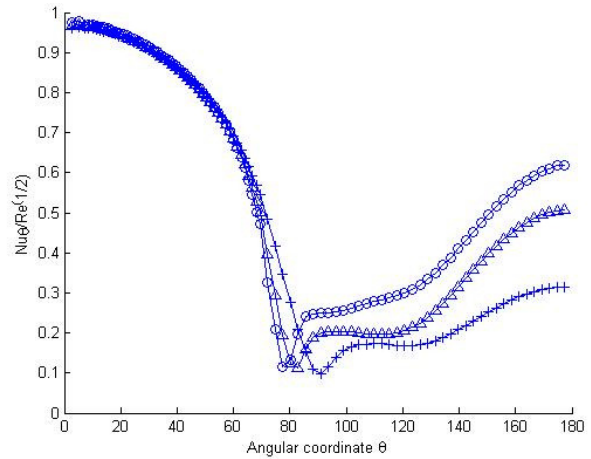


Figure 2 Local HTC at variable Re-number: +, *Re*=7407; Δ, *Re*=29630; o, *Re*=59259.

The empirical equation from Hilpert [10] is

$$\overline{Nu_D} = \frac{\bar{h}D}{k} = C\,Re^m\,Pr^{1/3} \tag{1}$$

where the constants C and m are listed in Table 1 for *Re* value ranges.

Table 1 Constants of Eq.(1) [10]

| Re | C | m |
|----|---|---|
| 4000-40,000 | 0.193 | 0.618 |
| 40,000-400,000 | 0.027 | 0.805 |

Table 2 compares the average Nusselt numbers obtained from empirical Eq. (1) and the numerical simulations. It can be seen that the numerical results are about 15% less than those from the empirical equation. The reason of this discrepancy is that the simulations were carried out at constant surface temperature, while most experiments were conducted at constant heat flux from the surface.

Table 2 overall average *Nu* for a circular cylinder

| Air Velocity(m/s) | Re | Nu_Eq.1 | Nu(numerical) |
|---|---|---|---|
| 1 | 7407 | 42.90 | 39.59 |
| 4 | 29630 | 101.04 | 86.46 |
| 8 | 59259 | 169.85 | 133.03 |

A mixture of ice particles and water are produced during the snow melting process, so it is better to choose a model at a constant surface temperature of 0 °C.

### IV.  HEAT TRANSPORT OF A ELLIPTICAL CYLINDER

*Elliptical cylinder definition*

An ellipse is a smooth closed curve which is symmetric about its center. The distance between antipodal points on the ellipse (pair of points whose midpoint is at the center of the ellipse) is maximum and minimum along two perpendicular

directions, the major axis (transverse diameter) and the minor axis (conjugate diameter) respectively. The semimajor axis or major radius (denoted by *a* in Figure 3) and the semiminor axis or minor radius (denoted by *b* in Figure 3) are one half of the major and minor diameters, respectively.
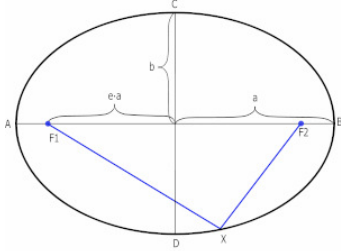


Figure 3 ellipse definition

1. The eccentricity of the ellipse is

$$e = \sqrt{1 - \left(\frac{b}{a}\right)^2}$$
(2)

2. The flatness ratio is defined as

$$f = \frac{a}{b}$$
(3)

3. The area enclosed by the ellipse is

$$A = \pi ab$$
(4)

where *a* and *b* are one-half of the ellipse's major and minor axes respectively.

4. circumference

A good approximation of circumference is Ramanujan's equation:

$$C \approx \pi \left[ 3(a+b) - \sqrt{(3a+b)(a+3b)} \right]$$
(5)

*Snow sleeve deformation*

It is assumed that the area of the snow sleeve keeps constant during the snow melting process. The deformation factor is defined as

$$d = \frac{\Delta l}{R}$$
(6)

Where $R$ is the radius of the circular shape, and $\Delta l$ is the variation in length of the semiminor radius of ellipse.
So, the semiminor radius can be obtained by

$$a = R \times (1 - d)$$
(7)

and the semimajor radius by

$$b = A / (\pi \times a)$$
(8)

The parameters of a set of ellipses are listed in Table 3. From this, it is obvious that the perimeter of ellipse increase with its eccentricity.

It should be noted that snow sleeve becomes deformed as a bluff shape, i.e. when the major axis is perpendicular to the flow.

Table 3 Ellipse parameters

| d | a | B | Perimeter | e | f |
|------|--------|--------|-----------|------|------|
| 1% | 0.0495 | 0.0505 | 0.3140 | 0.20 | 0.98 |
| 5% | 0.0475 | 0.0526 | 0.3146 | 0.43 | 0.90 |
| 10% | 0.0450 | 0.0556 | 0.3166 | 0.59 | 0.81 |
| 20% | 0.0400 | 0.0625 | 0.3257 | 0.77 | 0.64 |
| 30% | 0.0350 | 0.0714 | 0.3440 | 0.87 | 0.49 |

*Local HTC distribution*
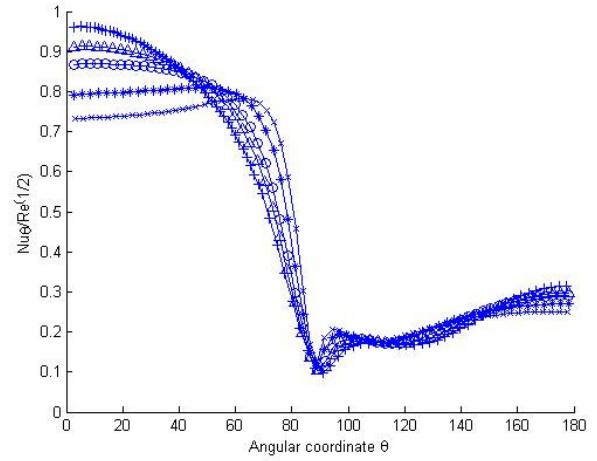


Figure 4. Local HTC at Re-number=7407 and variable eccentricity e: +, e=0; Δ, e=0.43; o, e=0.59; *, e=0.77; x, e=0.87.
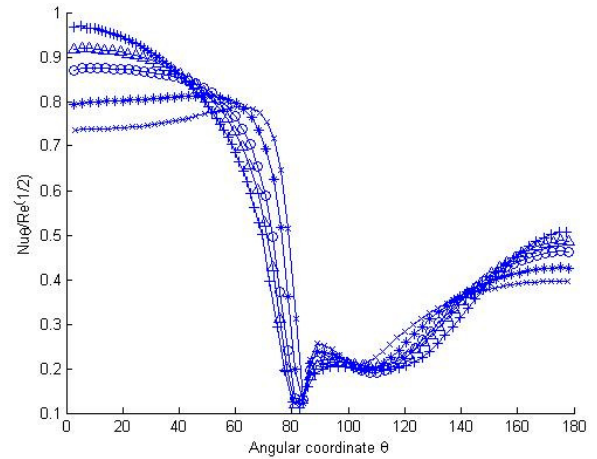


Figure 5. Local HTC at Re-number=29630 and variable eccentricity e: +, e=0; Δ, e=0.43; o, e=0.59; *, e=0.77; x, e=0.87.

Figure 4, Figure 5 and Figure 6 show the numerical results for a set of elliptical cylinders. The parameter varied here is surface roughness, and the Nusselt number is normalized by $Re^{-1/2}$.

Figure 4 shows the results associated with the smallest Reynolds number, $Re$=7407. The curves have similar shape when the deformation factor is less than 10%: the maximum $Nu$ is near the front stagnation point, and the separation point is at around θ=80°.
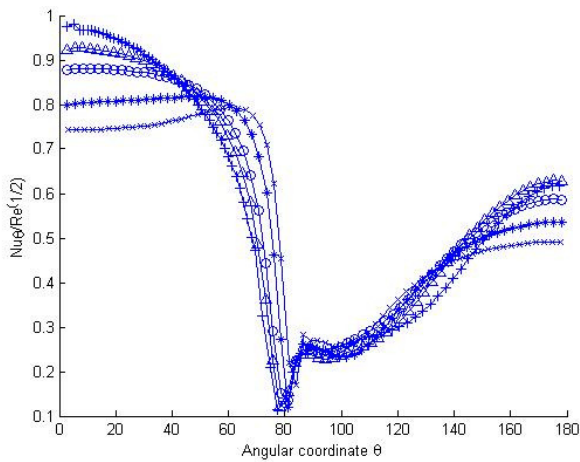
Figure 6. Local HTC at Re-number=59259 and variable eccentricity e: +, e=0; Δ, e=0.43; o, e=0.59; *, e=0.77; x, e=0.87.

It is seen that the *Nu* value near the front stagnation point decreases with the increasing ellipse's eccentricity, i.e. the increasing of deformation. For higher deformation range (factor> 10%), the maximum *Nu* occurs at about θ=70° which is close to separation point.

The major reason for that is the difference in geometry between the circle and the ellipse. The curvature of an ellipse is not uniform along its boundary: at θ=0° (near the front stagnation point) or θ=180° the curvature has minimum value, at θ=90° or θ=270° the curvature reaches its maximum value. Also, an ellipse's perimeter is longer than a circle's. So at θ=0°, an elliptical cylinder shows more analogical features with a plate which is perpendicular to the air flow than a circular cylinder does. Furthermore, the higher eccentricity, the smaller curvature is at θ=0°. So, the value of *Nu* at θ=0° decreases as eccentricity increases.

In the wake region, the air flow is full of vortices, and does not have a unity direction, so that the effects occurring there are much less important than those in the laminar boundary layer.

At a given Reynolds number, it can also be found that:
- The separation point moves downward with increasing eccentricity.
- The value of *Nu* at the separation point increases as the eccentricity increases.

Margarita Baevay et al. (1997) proposed a theoretical analysis of the heat transfer from a moving elliptical cylinder, but the Peclet number selected in the paper is less than 2.5 which is too small for snow sleeve issues. Anyhow, some similar characteristics can be found: the lower value at θ=0° and the maximum is around θ=70°.

*Overall heat transfer*

A. Zukauskas et al (1985) reported on the external heat transfer for a single elliptical cylinder in cross flow. They focused their investigation on an elliptical cylinder whose flatness ratio is 0.52. The cylinder was aligned with the major axis parallel and perpendicular to the flow. They proposed a correlation that describes the average external heat transfer for elliptic cylinders:

$$Nu_{dl} = 0.27 Re_{dl}^{0.6} Pr^{0.37} \left(\frac{Pr}{Pr_W}\right)^{0.25}$$

(9)

Where $Nu_{dl}$ is the overall average Nusselt number, Pr and $Pr_w$ are the Prantdl number of air and near the wall, respectively. For the bluff elliptical body flow, dl is 2 times major axis.

This correlation was derived for the boundary condition of UHF and is valid over the range of $2 \times 10^4 \leq Re_{dl} \leq 2 \times 10^5$.

Daniel K. Harris and Victor W. Goldschmidt (2002) carried out experiments in wind tunnel and reported results for three flatness ratios, 0.20, 0.31, and 0.52, in addition to three incidence angles, 0, 45, and 90 degrees.

However, flatness ratios less than 0.80 mean enormous deformation for snow sleeves which could not happen in reality. Nevertheless, it is still a good way to verify the validation of numerical methods by comparing results.

From Eq. (9), it is possible to obtain the Nusselt number, $Nu_{ell}$ for an elliptical cylinder at flatness ratio = 0.52, which is about 92% of that for a circular cylinder. From Table 4, the numerical results for an elliptical cylinder at flatness ratio=0.49 show that the ratio is around 95%, a little higher than the Zukauskas and Ziugzda's data.

Table 4. *Nu* for circular and elliptical cylinder

|  | e=0 | e=0.87 | Ratio |
|---|---|---|---|
| *Re*=7407 | 39.59 | 37.69 | 95% |
| *Re*=29630 | 86.46 | 83.01 | 96% |
| *Re*=59259 | 133.03 | 126.22 | 94% |

Figure 7 and Table 5 show the overall heat transfer around the elliptical cylinder. It can be observed that the heat-transfer coefficient stays almost constant at eccentricity <0.6, and decreases abruptly when eccentricity >0.8.

Table 5. Overall HTC at variable Reynolds number

| E | 0 | 0.20 | 0.34 | 0.43 | 0.59 |
|---|---|---|---|---|---|
| *Re*=7407 | 39.59 | 39.58 | 39.53 | 39.40 | 39.21 |
| *Re*=29630 | 86.46 | 85.95 | 86.37 | 86.77 | 85.68 |
| *Re*=59259 | 133.03 | 132.92 | 132.20 | 133.20 | 134.01 |
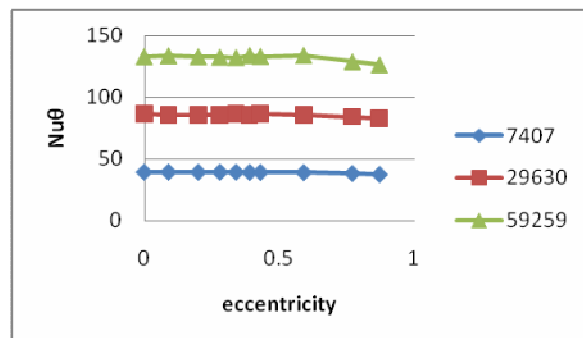


Figure 7. Overall HTC at variable Reynolds number

## V. FORCED HEAT TRANSFER OF A ROUGH SURFACE CYLINDER

### Roughness of snow

P. Lacrox et al. (2008) has investigated snow pack and found that the roughness of snow varied in a large range due to weather and geography conditions. Even for relatively smooth surfaces, the classical roughness parameters are found to be in the 0.5-9.2mm range for the RMS height distribution. For more detailed information on the rough surface effects, a set of values are listed in Table 6.

Table 6. Roughness parameters

| Roughness Height(m) | Diameter(m) | $K_s/D(10^{-3})$ |
|---|---|---|
| 0.000075 | 0.1 | 0.75 |
| 0.00009 | 0.1 | 0.9 |
| 0.0001 | 0.1 | 1 |
| 0.0005 | 0.1 | 5 |
| 0.001 | 0.1 | 10 |
| 0.002 | 0.1 | 20 |
| 0.003 | 0.1 | 30 |
| 0.004 | 0.1 | 40 |

The roughness constant is set as 0.5 in Fluent.

### Local HTC distribution

In Figure 8, Figure 9 and Figure 10, the local heat-transfer distribution around a cylinder is plotted for each Reynolds number. The parameter varied here is surface roughness. The Nusselt number is normalized by $Re^{-1/2}$.

Figure 8 shows the results for the smallest Reynolds number, $Re$=7407. It can be seen that most of affects caused by surface roughness occurs in the wake range of the air flow. Even at the highest roughness value, $K_s/D$=50×10⁻³, the minimum $Nu$ is still at almost same position as for a smooth surface.
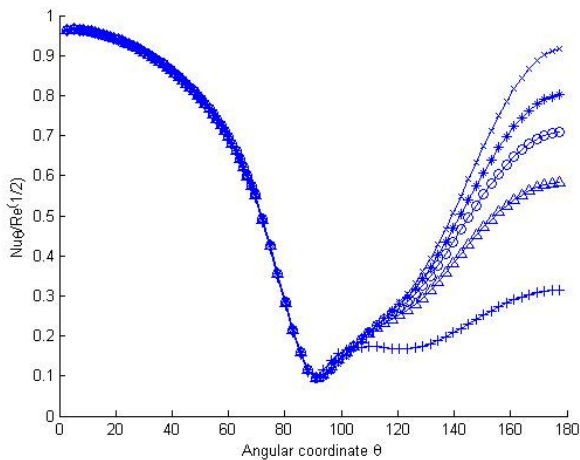


Figure 8. Local HTC at Re-number=7407 and variable roughness r= k$_s$/d: +, r=0, smooth surface; Δ, r=10*10⁻³; o, r=30×10⁻³, *, r=40×10⁻³; x, r=50×10⁻³.
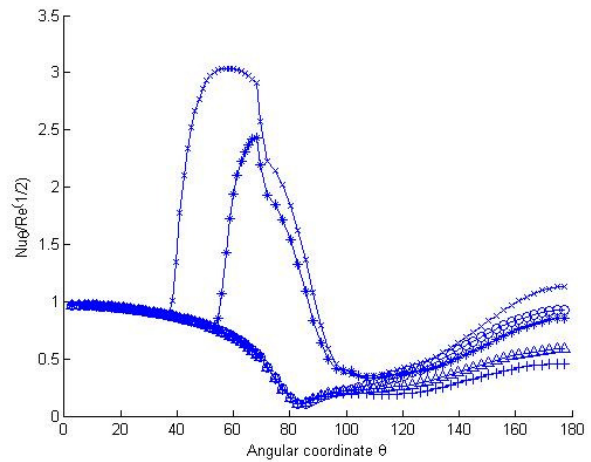


Figure 9. Local HTC at Re-number=2.2×10⁴ and variable roughness r= k$_s$/d: +, r=0, smooth surface; Δ, r=12×10⁻³; o, r=20×10⁻³, *, r=30×10⁻³; x, r=35×10⁻³
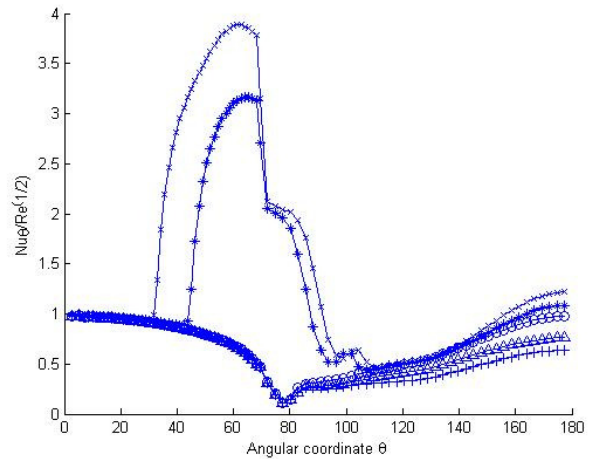


Figure 10. Local HTC at Re-number=6.67×10⁴ and variable roughness r= k$_s$/d: +, r=0, smooth surface; Δ, r=3×10⁻³; o, r=9×10⁻³, *, r=12×10⁻³; x, r=1.5×10⁻³

Figure 9 exhibits the results for a higher Reynolds number, $Re$=22222. In a lower roughness range $K_s/D$<2×10⁻², the curves have similar shape characteristics: the boundary layer is laminar throughout, and its separation is indicated by a minimum near θ=80°.

When the curve is associated with higher roughness $K_s/D$=3×10⁻² is compared to that with a smooth surface, the difference is apparent. There is a direct transition from laminar to turbulent boundary layer at 50°, generating high heat transfer coefficients downstream because the heat transfer in the turbulent flow is more effective than in the laminar flow. In the turbulent region, $Nu$ increases with increasing θ until it reaches its maximum value at around θ≈70°, and then decreases. The separation occurs at θ≈110°. The curve $K_s/D$=1.5×10⁻² shows a similar behavior with the exception that the transition point is at θ≈40°, and the peak value of the Nusselt number is about 23% higher.

Figure 10 qualitatively shows similar results for the local heat transfer at $Re$=66667. Comparing Figure 10 and Figure 9, it is observed that as the roughness parameter is increased, the laminar-turbulent transition occurs at a decreasing Reynolds

number.

The values of heat transfer at the front stagnation point should be expected to be equal to unity, as the flow near the stagnation point is laminar. Some experimental results are greater than unity due to the limitation of laboratory equipment.

Lasse Makkonen (1985) developed a mathematical boundary-layer model to predict the local HTC distribution along a rough cylinder surface. E. Achenbach (1976) designed a series of tests to obtain heat transfer on a rough surface. The numerical results are in good agreement with their conclusion.

*Overall heat transfer*

Figure 11 exhibits the overall average Nusselt numbers at different roughness value. It is can be seen that the total heat-transfer increases with increasing roughness. After roughness parameter exceed a critical value, heat transfer increases more intensely. But at lower *Re* there is no such critical value.
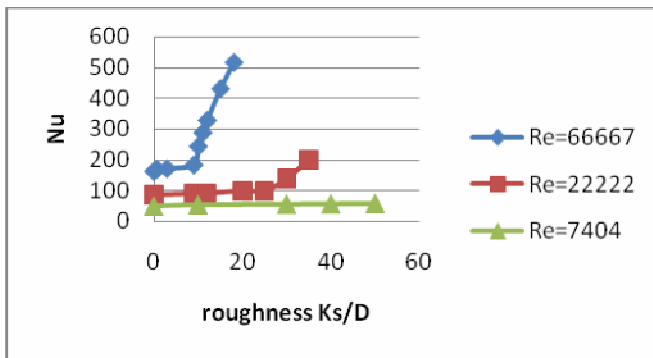


Figure 11 Overall average HTC at variable roughness

## VI. CONCLUSION

From the discussion of the results on the elliptical shape cylinder, the effects from sleeve deformation can be neglected if eccentricity <0.6. Snow shedding from overhead cables will occur when eccentricity reaches a critical value, which usually is very small in reality climatic situation. So in most cases, the effects of sleeve shape on snow shedding will be negligible.

The numerical results taking roughness effects into account are in good agreement with experiments. However, our investigation demonstrate that roughness has a significantly effect on heat transfer rate.

At a given Reynolds number, it is can be seen that:

● The higher the roughness, the closer the laminar-turbulent transition point approaches the front stagnation point.
● The peak value of *Nu* increases as the roughness parameter increases.
● The heat-transfer within the wake region increases with increasing roughness.

Unfortunately, it is difficult to measure the variation in roughness during the snow melting process. The snow sleeve will not melt at an uniform rate if density is not homogeneous. The outer wind and water flow within the snow will also affect the variation in roughness. It was found that roughness increase more rapidly at the upper part of the snow sleeve.

Further investigations are needed to study the effects of snow roughness.

## VII. ACKNOWLEDGEMENTS

## VIII. REFERENCES

*Periodicals:*

[1] A. Zhukauskas, J. Ziugzda, Heat Transfer of a Cylinder in Cross-flow, Hemisphere Publishing Co., Washington, DC, 1985.
[2] Daniel K. Harris, Victor W. Goldschmidt, Measurements of the overall heat transfer from combustion gases confined within elliptical tube heat exchangers, Experimental Thermal and Fluid Science 26 (2002) 33–37.
[3] E. Achenbach, Total and local heat transfer from a smooth circular cylinder in cross-flow at high Reynolds number, Int. J. Heat Mass Transfer 18. P1387-1396, 1975.
[4] E. Achenbach, the effect of surface roughness on the heat transfer from a circular cylinder in cross-flow at high Reynolds number, Int. J. Heat Mass Transfer 20. P359-369, 1977.
[5] Ertan BUYRUK, Heat Transfer and Flow Structures Around Circular Cylinders in Cross-Flow, Int. J. of Engineering and Environmental Science, 23 (1999) , 299-315.
[6] J. W. SCHOLTEN and D. B. MURRAY, Unsteady heat transfer and velocity of a cylinder in cross flow- I. Low freestream turbulence, Int. J. Heat Mass Transfer, Vol. 41, No. 10, 1139-1148, 1998
[7] Lasse Makkonen, Heat transfer and icing of a rough cylinder, Cold Regions Science and Technology, 10(1998)105-106.
[8] Lacroix, P.; Legrésy, B.; Langley, K.; Hamran, S.E.; Kohler, J.; Roques, S.; Rémy, F.; Dechambre, M, In situ measurements of snow surface roughness using a laser profiler, Journal of Glaciology, Volume 54, Number 187, December 2008 , pp. 753-762(10)
[9] Margarita Baevay, Plamen Baevz and Alexander Kaplanx, An analysis of the heat transfer froma moving elliptical cylinder, J. Phys. D: Appl. Phys. 30 (1997) 1190–1196.

*Books:*

[10] Frank P. Incropera, Fundamentals of heat and mass transfer, 6th ed., Hoboken, N.J. : J. Wiley, 2007.

*Dissertations:*

[11] Zsolt Peter : « Modelling and Simulation of the Ice Melting Process on a Current-Carrying Conductor », PhD in Engineering, UQAC, April 2006

*Technical Reports:*

[12] Flow Over a Cylinder, Fluend Inc., April 16, 2007

*Papers from Conference Proceedings (Published):*

[13] K. Szczepanik, A. Ooi1, L. Aye and Gary Rosengarten, A Numerical Study of Heat Transfer from a Cylinder in Cross Flow, 15th Australasian Fluid Mechanics Conference, The University of Sydney, Sydney, Australia, December 2004.